Supplement of Solid Earth, 9, 797–819, 2018
https://doi.org/10.5194/se-9-797-2018-supplement

Solid Earth Open Access EGU

Supplement of

Ca-rich garnets and associated symplectites in mafic peraluminous granulites from the Gföhl Nappe System, Austria

Konstantin Petrakakis et al.

Correspondence to: Konstantin Petrakakis (konstantin.petrakakis@univie.ac.at)

XRF-analyses of rocks and normative recalculation

The collected samples were crashed, dried at 110°C and then calcined at 1050°C for the calculation of the loss of ignition (LOI) and the preparation of fused pellets diluted (1:5) with $Li_2B_4O_7$. Major elements measurements were performed with a Philips PW2400 spectrometer at the Department of Lithospheric Research, University of Vienna. The analyses below are recalculated based on LOI and the oxygen balance resulting from the transformation of total Fe as Fe_2O_3 (formed during calcination) to total FeO.

Normative contents are based on cation-equivalents. They are calculated as follows. The weight-% of each oxide was divided by its cation equivalent weight (molar mass of each oxide or mineral formula divided by the number of cations involved). The resulting cation proportions were normalized to 100% forming thus an input vector. The latter was then recast in normative minerals by multiplication with the inverse transformation matrix formed either by the mineral column vectors (*ap , il, or, ab, crn, di, hy, ol*) or (*ap, il, or, ab, an, crn, di, hy*). Thereby, X_{mg} of *di, hy, ol* was set equal with the bulk rock X_{mg}.

The justification and benefits of the cation-equivalent norm especially for metamorphic rocks are described in Burri (1959) and Barth (1962). Particularly, the resulting cation-normative contents reflect the approximate weight-% of the minerals.

Microprobe analyses and formula recalculation

Mineral point analyses were performed at the Department of Lithospheric Research, University of Vienna with a CAMECA SX100 microprobe using wave length and energy dispersion facilities and natural minerals as reference materials. The analyses were then processed with the latest version of the program MINSORT (Petrakakis & Dietrich, 1985). The adopted formula recalculation methods are as follows.

1. Clinopyroxene and orthopyroxene formula is based on 6 Oxygens per formula unit (p.f.u.). If the sum of cations exceeds the stoichiometric sum, Fe^{3+} is calculated by iterating the molar ratio Fe_2O_3/FeO until the Cation Sum = 4. Cation assignment to sites follows Morimoto et al. (1988).

2. Garnet formula is based on 12 Oxygens p.f.u. If the sum of cations exceeds the stoichiometric sum, Fe^{3+} is calculated by by iterating the molar ratio Fe_2O_3/FeO until the site occupancy in site M = 2.

3. Amphibole formula follows Schumacher in Leake et al. (1997). The tabulated analyses below are the average of the two feasible solutions corresponding to maximum and minimum Fe^{3+} not violating amphibole stoichiometry.

4. Feldspar formula is based on 8 Oxygens p.f.u. If appropriate, Fe^{3+} is put into the tetrahedral site Z.

5. Spinel formula is based on 32 Oxygens p.f.u. If the sum of cations exceeds the stoichiometric sum, Fe^{3+} is calculated by iterating the molar ratio Fe_2O_3/FeO until the Cation Sum = 24.

The analyses given in the following tables are average analyses over enough point analyses of the same mineral kind, occurrence and features. The abbreviations m(n) and ±s shown over the analyses columns denote the Mean of n point analyses and their Standard Deviation, respectively.

Bulk chemical composition of crack symplectites

Several BSE images of various crack- symplectites have been repeatedly analyzed and used for the calculation of the bulk symplectite composition (e.g. Paper, Fig. 4b). In each image, the area of each symplectitic phase shows a distinct gray-color value. The distribution of each color in each image is a measure of the area proportion of the phase. Color distribution of each out of seven different symplectite images has been acquired over six timely independent sessions with the aid of the open-access software *ImageJ* (https://imagej.net/Welcome). The underlying assumption is that the phase area distributions reflect the phase volume distribution. The results are summarized in Table S1.

The distinction between orthopyroxene and clinopyroxene was not easy, as both phases showed very similar gray colors. The accompanying Ca-distribution maps showed however that ~3% of the pyroxene areas were clinopyroxene. Several averaged microprobe analyses of each symplectitic phase (see Table S 6) helped further calculate the phase densities as sums of tabulated endmember densities weighted by their molefractions. Endmembers calculation from phase analyses has been carried out by considering total Fe as Fe^{2+} + Mn. Minor elements like K, Ti, Cr etc. have been ignored. The utilized endmembers are the following.

Table S 1. Measured volumes of phases in crack symplectites.

Phase	Vol-%	
	m(42)	±s
OPX	37.9	4.3
CPX	1.2	
SPL	12.3	0.9
PL	40.3	4.4
HBL	8.3	2.7
Total	100.0	

GRT: *alm, prp, grs*; OPX: *en, fs, di, ortho-crn*; CPX: *di, hd, cTs, en, fs*;
SPL: *spl, hrc*; PL: *an, ab.*

Densities have been calculated from molar volume and weight data in Robie & Hemingway (1995) and, for *ortho-crn* from Berman & Aranovich (1996). Finally, the formula below allowed for the calculation of each oxide wt-% of the bulk symplectite.

$$w_i^s = \sum_j \left[w_i^j \cdot \left[v^j \cdot \sum_k \left(X_k^j \cdot \rho_k^j \right) \right]_{\%} \right]$$

k : over endmembers in phase j.
j : over phases in symplectite s.
i : over oxides in phase j.

X_k^j : molefraction of k in j.
ρ_k^j : density of k in j.
v^j : measured volume of j.
w_i^j : mesured wt-% of oxide i.
w_i^s : bulk wt-% of oxide i in symplectite.

The calculated oxide values for the bulk symplectite have been then subtracted from those of the initial garnet (cf. in paper Fig. 5e).

Electron Backscatter Diffraction (EBSD) analyses

Electron Backscatter Diffraction (EBSD) analysis have been collected using an FEI Quanta 3D FEG electron microscope at the Faculty of Earth Sciences, Geography and Astronomy at the University of Vienna (Austria). The instrument is equipped with a Schottky-type field emission electron source for electron beam microanalysis and imaging at high spatial resolution. Several signal detection systems have been utilized, comprising an Everhart-Thornley secondary electron detector (SED) for mineral phase distribution and 2D interface geometry imaging, a fore-scattered electron detector (FSD) for orientation contrast imaging, and an EDAX Digiview IV EBSD camera for crystallographic orientation mapping. During EBSD data collection, additionally qualitative major element composition information was obtained from energy-dispersive X-ray spectrometry using an Apollo XV Silicon Drift Detector. Still, EBSD indexing and phase identification are exclusively based on the crystal structure. During EBSD analyses, electron beam settings have been set at 15kV accelerating voltage and approximately 4 nA probe current using the analytic (high current) electron beam mode at the smallest possible spot size. The chemo-mechanically polished thin section surface was tilted to 70° (beam incidence angle 20°) at a working distance of 14 mm. The OIM Data Collection Software v6.2 (update 23.10.2012) was used for EBSD data acquisition, whereas the OIM Analysis Software v7.3.0 as well as the Matlab-toolbox MTEX have been used for data evaluation and plotting. The EDAX Digiview IV EBSD camera, which is mounted at 5° elevation angle, was set to 4x4 binning and 95 milliseconds exposure time for single frame EBSD pattern collection during crystal orientation mapping. Both static and dynamic background corrections and a histogram intensity normalization filter have been applied to optimize EBSD pattern contrast. Hough settings for automated band detection have been set at 160 pixels binned pattern size, 1° θ step size, and 80% rho-fraction, using a 9 × 9 pixels convolution mask to index 3-17 reflectors with a minimum peak distance of 7 pixels. Band center positions have been used for EBSD pattern indexing at an inter-planar tolerance angle of 2°. The crystal orientation data shown in Fig. S1 are collected from a 65 × 53 nm sized scan area in hexagonal grid mode at a step size of 150 nanometers. In order to remove mis-indexed points a series of clean-up procedures has been applied using the OIM Analysis software v 7.3. First, the Grain Confidence Index Standardization procedure has been employed (grains defined by a tolerance angle of 5° between neighbor points, having a minimum grain size of 2 data points and comprising data of more than one scan row). Secondly, the Neighbor Orientation Correlation clean-up procedure has been applied, whereby the orientation of a point is changed according to the orientation of 4 equally oriented neighbor points (grain tolerance angle 5°, minimum confidence index 0.1). This second cleanup step caused data orientation modification of 1.96 % of the data points. Finally, one iteration of a Dilation Clean-up has been

run in order to remove mis-indexed points at grain or phase boundaries and adjacent to pores. This step caused data modification of 4.67 % of the data points. The clean-up procedures highly increased the number of points with confidence index > 0.1 to 99.3 % of all data points of this scan.

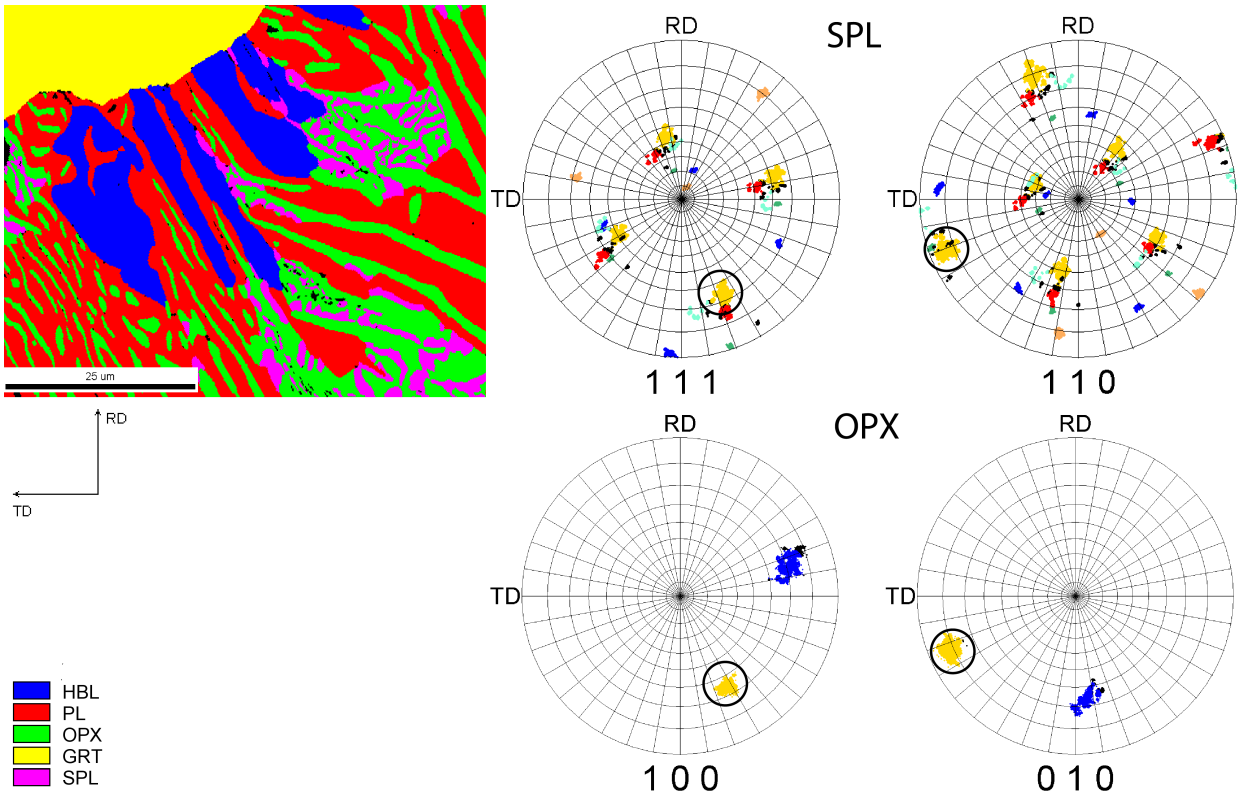

Figure S 1. Phase identification map showing garnet at the contact to rim-symplectite and pole figures for spinel and orthopyroxene in the symplectite. A a clear rational orientation relation is identified only between spinel and orthopyroxene with $(111)_{SPL} \parallel (100)_{OPX}$ and $(110)_{SPL} \parallel (010)_{OPX}$. No rational orientation relations can be detected with the reactant garnet, nor with the plagioclase and hornblende of the symplectite.

References

Barth T. F. W. (1962): Theoretical petrology. John Wiley & Sons, New York.

Berman, R.G. and Aranovich, L.Y. (1996). Optimized standard state and solution properties of minerals: I. Model calibration for olivine, orthopyroxene, cordierite, garnet, and ilmenite in the system FeO-MgO-CaO-Al_2O_3-TiO_2-SiO_2. Contributions to Mineralogy and Petrology, 126, 1–22.

Burri C. (1959): Petrochemische Berechnungsmethoden auf äquivalenter Grundlage.- Birkhäuser Verlag, Zürich.

Leake et al. (1997). Nomenclature of amphiboles: Report of the Subcommittee on Amphiboles of the International Mineralogical Association, Commission on New Minerals and Mineral Names. American Mineralogist, 82, 1019-1037.

Morimoto et al. (1988). Nomenclature of pyroxenes. Mineralogical Magazine 52, 535-550.

Petrakakis, K. and Dietrich, H. (1985). MINSORT: A program for the processing and archivation of microprobe analyses of silicate and oxide minerals. Neues Jahrbuch für Mineralogie, Mh. 1985 (8), 379-384.

Robie, R. A. and Hemingway, B. S. (1995). Thermodynamic properties of minerals and related substances at 298.15 K and 1 Bar (10^5 Pascals) Pressure and at higher temperatures. U. S. Geological Survey Bulletin 2131, Washington

Tables of analyses

Table S 2. XRF- rock analyses and normative composition of the selected samples.

Wt.-%	Samples						
	UM_4	UM_5	UM_6	UM_9	**UM_8**	UM_10	UM_11
SiO_2	47.133	46.675	47.658	45.955	**46.116**	47.958	48.750
TiO_2	0.371	0.121	0.090	0.232	**0.210**	0.422	0.171
Al_2O_3	17.809	15.186	15.062	16.520	**22.364**	19.352	15.557
FeO	6.006	7.226	5.931	8.466	**3.433**	6.214	7.130
MnO	0.110	0.161	0.121	0.171	**0.060**	0.110	0.161
MgO	10.844	15.266	13.414	11.343	**9.033**	8.311	11.670
CaO	14.832	13.777	15.796	15.191	**16.332**	14.614	14.623
Na_2O	1.864	1.006	1.537	1.289	**1.273**	2.178	1.165
K_2O	0.110	0.040	0.040	0.161	**0.235**	0.060	0.110
P_2O_5	0.020	0.030	0.010	0.040	**0.015**	0.020	0.020
H_2O (LOI)	0.451	0.171	0.181	0.212	**0.519**	0.321	0.362
Total	99.550	99.660	99.840	99.580	**99.590**	99.560	99.720
Cation equivalent norm							
ap	0.041	0.062	0.021	0.084	**0.031**	0.042	0.042
il	0.510	0.165	0.123	0.321	**0.289**	0.583	0.236
or	0.643	0.233	0.232	0.945	**1.370**	0.353	0.648
ab	16.526	8.838	13.487	11.494	**11.293**	19.418	10.381
an	0.000	0.000	0.000	0.000	**18.779**	9.500	11.687
crn	15.761	14.399	13.321	15.416	**14.071**	13.221	9.972
di	58.032	53.333	61.212	59.657	**48.942**	49.897	48.151
hy	5.748	15.093	2.538	5.625	**5.225**	6.986	18.883
ol	2.738	7.878	9.067	6.458	**0.000**	0.000	0.000
Total	100.000	100.000	100.000	100.000	**100.000**	100.000	100.000
X_{mg}	0.760	0.786	0.798	0.701	**0.822**	0.701	0.740

Table S 3. Garnet type compositions. The given garnet type compositions are average compositions of several consecutive point analyses of largely uniform composition along the garnet profile Z1-Z2-Z3 in Paper, Fig. 5a. The component distributions of the averaged microprobe analyses are shown in Fig. S2. The abbreviation n.a. designates "not analyzed".

GRT	Type Z1		Type Z2		Type C		Type Z3		Type E		Contact		Initial, #974
	m (50)	±s	m (33)	±s	m (30)	±s	m (21)	±s	m (18)	±s	m (24)	±s	
SiO2	41.475	0.178	40.754	0.660	40.889	0.114	40.867	0.124	41.605	0.185	40.083	0.277	41.602
TiO2	0.043	0.015	0.095	0.024	0.090	0.014	0.132	0.020	0.073	0.025	0.045	0.028	0.057
Al2O3	23.702	0.151	23.420	0.494	23.501	0.095	23.379	0.079	23.519	0.149	22.777	0.126	23.431
Cr2O3	n.a.	n.a.	n.a.	n.a.	n.a.	n.a.	n.a.	n.a.	0.059	0.020	0.003	0.014	0.032
FeO	11.528	0.115	11.955	0.683	12.877	0.097	9.675	0.086	9.649	0.174	17.870	0.967	12.160
MnO	0.401	0.020	0.470	0.038	0.514	0.028	0.319	0.021	0.207	0.016	1.292	0.365	0.448
MgO	16.207	0.155	14.066	0.204	14.875	0.076	13.120	0.117	17.028	0.258	11.197	0.775	15.450
CaO	7.284	0.215	9.588	0.604	7.665	0.079	12.778	0.180	8.379	0.361	7.237	0.980	8.293
Total	100.639	0.343	100.348	1.083	100.412	0.234	100.271	0.211	100.518	0.324	100.503	0.284	101.473
Si	2.982		2.967		2.971		2.972		2.975		2.986		2.981
Al IV	0.018		0.033		0.029		0.028		0.025		0.014		0.019
Al VI	1.990		1.977		1.984		1.976		1.957		1.986		1.960
Cr	0.000		0.000		0.000		0.000		0.003		0.000		0.002
Ti	0.002		0.005		0.005		0.007		0.004		0.003		0.003
Fe 3+	0.008		0.018		0.011		0.016		0.036		0.012		0.035
Fe 2+	0.685		0.710		0.772		0.572		0.541		1.101		0.694
Mn	0.024		0.029		0.032		0.020		0.013		0.082		0.027
Mg	1.737		1.527		1.612		1.423		1.815		1.243		1.650
Ca	0.561		0.748		0.597		0.996		0.642		0.578		0.637
T(3)	3.000		3.000		3.000		3.000		3.000		3.001		3.000
M(2)	2.000		2.000		2.000		2.000		2.000		2.001		2.000
C(3)	3.008		3.014		3.012		3.010		3.011		3.004		3.008
Xalm	0.228		0.236		0.256		0.190		0.180		0.367		0.231
Xsps	0.008		0.010		0.010		0.007		0.004		0.027		0.009
Xpyr	0.577		0.507		0.535		0.473		0.603		0.414		0.549
Xgrs	0.182		0.237		0.190		0.319		0.192		0.185		0.192
Xanr	0.005		0.011		0.008		0.012		0.020		0.007		0.019
Xuvr	0.000		0.000		0.000		0.000		0.001		0.000		0.001
Xmg	0.717		0.683		0.676		0.713		0.770		0.530		0.704
Recalculated values													
Fe2O3	0.141		0.326		0.197		0.298		0.666		0.319		0.652
FeO	11.401		11.662		12.700		9.407		9.049		19.181		11.574
Total	100.653		100.381		100.431		100.301		100.584		100.647		101.538

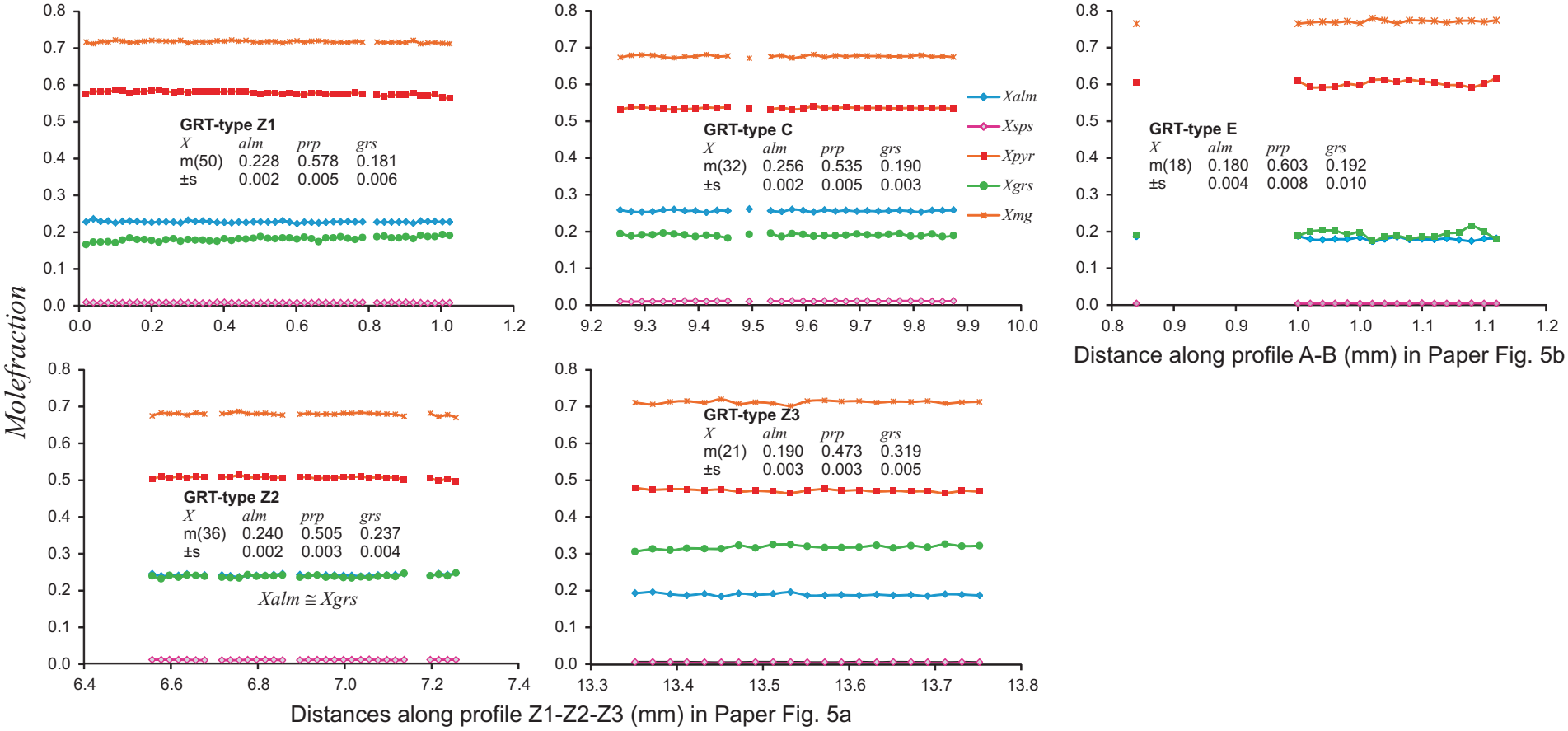

Figure S 2. Garnet profiles for garnet type definitions. The garnet profiles show the the largely uniform component distributions of several consecutive point analyses along the garnet profile Z1-Z2-Z3 in Paper, Fig. 6a, which have been averaged to the GRT-type analysis given in Table 2 and Table S3.

Table S 4. Microprobe analyses of CPX.

CPX	Matrix						CPX inclusions															
	Interior		Rim		Integral		GRT1,GRT2,GRT 3 UM8		Prof. E-F GRT3, UM8		Prof. A-B GRT3, UM8		Prof. C-D GRT3, UM8		Figs 11-17 GRT3, UM8		Prof. I-J UM8 (adj. Ky)		Prof. L-K GRT1, UM8		Poikiloblastic GRT in matrix of UM8A	
	m (20)	±s	m (2)	±s	m (120)	±s	m (9)	±s	m (3)	±s	m (7)	±s	m (8)	±s	m (4)	±s	m (32)	±s	m (26)	±s	m (3)	±s
SiO2	49.744	0.663	51.300	0.451	48.982	0.905	50.307	1.513	50.584	0.303	49.534	0.829	50.335	0.205	49.458	0.912	47.030	1.338	50.557	0.379	53.148	0.906
TiO2	0.461	0.043	0.341	0.001	0.465	0.054	0.416	0.255	0.270	0.018	0.610	0.062	0.243	0.022	0.643	0.081	0.891	0.168	0.229	0.083	0.152	0.105
Al2O3	9.282	1.265	5.773	0.374	10.294	0.954	8.673	3.967	8.207	0.215	9.425	1.280	8.090	0.458	9.311	1.209	14.604	1.715	7.765	0.465	3.303	0.886
Cr2O3	0.098	0.034	0.120	0.010	0.070	0.017	0.042	0.029	0.028	0.009	0.087	0.024	0.032	0.010	0.074	0.011	0.065	0.021	0.082	0.017	0.059	0.056
FeO	3.072	0.104	3.228	0.153	3.289	0.300	2.728	1.082	2.394	0.056	1.964	0.038	2.499	0.058	2.034	0.077	1.895	0.169	2.617	0.204	6.927	4.634
MnO	0.046	0.014	0.047	0.034	0.066	0.018	0.056	0.058	0.033	0.014	0.027	0.018	0.039	0.029	0.017	0.009	0.019	0.013	0.031	0.019	0.153	0.063
ZnO	0.009	0.015	0.012	0.017	0.023	0.025	0.010	0.018	n.a.		n.a.		n.a.		0.011	0.016	0.017	0.024	0.021	0.024	0.007	0.013
MgO	14.187	0.496	15.612	0.180	14.680	0.581	14.216	1.593	14.488	0.122	14.247	0.683	14.582	0.157	14.209	0.621	11.486	0.746	14.511	0.346	20.804	7.799
CaO	22.634	0.334	23.198	0.446	21.734	0.695	23.262	0.890	23.906	0.173	23.460	0.209	23.649	0.474	23.499	0.163	22.587	0.311	23.177	0.545	15.914	13.452
Na2O	0.866	0.109	0.601	0.016	0.783	0.122	0.722	0.595	0.520	0.027	0.726	0.053	0.527	0.045	0.674	0.033	1.262	0.051	0.748	0.108	0.218	0.191
K2O	0.006	0.006	0.005	0.000	0.013	0.009	0.009	0.008	0.002	0.004	0.016	0.012	0.006	0.006	0.020	0.019	0.034	0.065	0.023	0.019	0.001	0.002
Total	100.404	0.208	100.237	0.510	100.401	0.253	100.441	0.337	100.432	0.246	100.096	0.489	100.001	0.217	99.950	0.692	99.890	0.433	99.762	0.453	100.688	0.168
Si	1.796		1.857		1.764		1.817		1.827		1.791		1.825		1.792		1.704		1.836		1.905	
Al IV	0.204		0.143		0.236		0.183		0.173		0.209		0.175		0.208		0.296		0.164		0.095	
Fe 3+	0.000		0.000		0.000		0.000		0.000		0.000		0.000		0.000		0.000		0.000		0.000	
Al VI	0.191		0.103		0.201		0.186		0.177		0.192		0.171		0.190		0.328		0.169		0.044	
Fe 3+	0.047		0.060		0.062		0.024		0.017		0.032		0.027		0.029		0.008		0.033		0.056	
Ti 4+	0.013		0.009		0.013		0.011		0.007		0.017		0.007		0.018		0.024		0.006		0.004	
Cr	0.003		0.003		0.002		0.001		0.001		0.002		0.001		0.002		0.002		0.002		0.002	
Zn	0.000		0.000		0.001		0.000		0.000		0.000		0.000		0.000		0.000		0.001		0.000	
Mg	0.747		0.824		0.721		0.766		0.780		0.756		0.788		0.761		0.620		0.786		0.894	
Fe 2+	0.000		0.000		0.000		0.012		0.018		0.000		0.006		0.000		0.017		0.003		0.000	
Mn 2+	0.000		0.000		0.000		0.000		0.000		0.000		0.000		0.000		0.000		0.000		0.000	
Mg	0.016		0.019		0.067		0.000		0.000		0.012		0.000		0.006		0.000		0.000		0.218	
Fe 2+	0.046		0.038		0.037		0.047		0.037		0.027		0.043		0.033		0.032		0.043		0.151	
Mn 2+	0.001		0.001		0.002		0.002		0.001		0.001		0.001		0.001		0.001		0.001		0.005	
Ca	0.875		0.900		0.839		0.900		0.925		0.909		0.919		0.912		0.877		0.902		0.611	
Na	0.061		0.042		0.055		0.051		0.036		0.051		0.037		0.047		0.089		0.053		0.015	
K	0.000		0.000		0.001		0.000		0.000		0.001		0.000		0.001		0.002		0.001		0.000	
T(2)	2.000		2.000		2.000		2.000		2.000		2.000		2.000		2.000		2.000		2.000		2.000	
M1(1)	1.000		1.000		1.000		1.000		1.000		1.000		1.000		1.000		1.000		1.000		1.000	
M2(1)	1.000		1.000		1.000		1.000		1.000		1.000		1.000		1.000		1.000		1.000		1.000	
Xmg	0.943		0.957		0.955		0.929		0.934		0.966		0.941		0.959		0.926		0.945		0.880	

Table S 5. Microprobe analyses of PL and HBL.

PL	Matrix			Inclusion domains		Inclusions in poikiloblastic GRT			
	Interior		Rim	GRT3, UM8 GRT1, UM8A		Matrix GRT		Large GRT rim	
	m (8)	±s	m (2)	m (13)	±s	m (4)	±s	m (2)	±s
SiO2	49.286	0.224	46.758	45.465	0.154	47.588	0.492	51.851	0.081
TiO2	0.003	0.006	0.007	0.013	0.014	0.004	0.005	0.010	0.004
Al2O3	32.686	0.129	34.424	34.486	0.302	33.876	0.328	30.625	0.060
FeO	0.045	0.013	0.066	0.098	0.018	0.128	0.012	0.159	0.023
MnO	0.007	0.009	0.018	0.006	0.007	0.001	0.002	0.030	0.015
MgO	0.007	0.006	0.008	0.046	0.145	0.010	0.007	0.006	0.001
CaO	15.237	0.141	17.205	18.065	0.441	16.709	0.314	12.864	0.044
Na2O	3.088	0.078	1.871	1.224	0.070	2.237	0.158	4.382	0.124
K2O	0.019	0.010	0.021	0.138	0.214	0.019	0.008	0.026	0.004
Total	100.378	0.213	100.377	99.540	0.511	100.573	0.235	99.952	0.182
Si	2.243		2.141	2.106		2.171		2.355	
Al IV	1.753		1.857	1.882		1.822		1.639	
Fe 3+	0.002		0.003	0.004		0.005		0.006	
Ti	0.000		0.000	0.000		0.000		0.000	
Fe2+	0.000		0.000	0.000		0.000		0.000	
Mn	0.000		0.001	0.000		0.000		0.001	
Mg	0.000		0.001	0.003		0.001		0.000	
Ca	0.743		0.844	0.896		0.817		0.626	
Na	0.272		0.166	0.110		0.198		0.386	
K	0.001		0.001	0.008		0.001		0.002	
Z(4)	3.998		4.001	3.992		3.998		4.001	
X(1)	1.017		1.012	1.018		1.017		1.015	
an	0.731		0.835	0.884		0.804		0.618	
ab	0.268		0.164	0.108		0.195		0.380	
or	0.001		0.001	0.008		0.001		0.002	

HBL	Inclusion domains				Matrix	
	GRT3 (AB), UM8		GRT1 (IJ; adj. Ky), UM8		Prof. CD, UM8A	
	m (11)	±s	m (8)	±s	m (7)	±s
SiO2	41.749	0.845	40.751	0.265	43.290	0.126
TiO2	1.501	0.473	1.460	0.138	1.298	0.027
Al2O3	18.363	1.932	20.548	0.108	15.090	0.136
Cr2O3	0.071	0.016	0.054	0.020	0.236	0.027
FeO	3.436	1.171	3.733	0.383	5.806	0.065
MnO	0.026	0.033	0.020	0.016	0.060	0.011
MgO	16.393	0.953	15.070	0.075	16.839	0.090
CaO	12.411	0.249	12.355	0.347	12.172	0.059
Na2O	1.824	0.446	1.799	0.116	2.997	0.059
K2O	1.812	0.617	1.349	0.103	0.246	0.015
Total	97.587	0.542	97.139	0.361	98.034	0.220
Si	5.919		5.789		6.131	
Al_IV	2.081		2.211		1.869	
Ti	0.000		0.000		0.000	
Al_VI	0.987		1.230		0.650	
Ti	0.160		0.156		0.138	
Cr	0.008		0.006		0.026	
Fe_3+	0.106		0.103		0.226	
Mg	3.465		3.192		3.555	
Fe_2+	0.274		0.314		0.405	
Mn	0.000		0.000		0.000	
Mg	0.000		0.000		0.000	
Fe_2+	0.027		0.027		0.057	
Mn	0.003		0.002		0.007	
Ca	1.885		1.881		1.847	
Na	0.085		0.090		0.088	
Na	0.417		0.405		0.735	
K	0.328		0.245		0.044	
T(8)	8.000		8.000		8.000	
C(5)	5.000		5.000		5.000	
B(2)	2.000		2.000		2.000	
A(0-1)	0.744		0.650		0.779	
Xmg	0.920		0.904		0.885	

Table S 6. Averaged microprobe analyses of CPX, OPX, SPL and PL in crack-symplectite, see Paper, Figs. 4c,d.

	OPX		CPX		Contact-GRT		SPL		PL		HBL (late)	
	m (46)	±s	m (13)	±s	m (24)	±s	m (30)	±s	m (60)	±s	m (32)	±s
SiO2	53.46	0.50	52.26	1.13	40.083	0.277	0.34	0.53	44.18	0.31	42.49	0.58
TiO2	0.04	0.03	0.24	0.17	0.045	0.028	0.02	0.01	0.01	0.01	0.74	0.32
Al2O3	3.37	0.66	3.40	1.41	22.777	0.126	63.65	0.64	35.34	0.49	16.02	0.69
Cr2O3	0.03	0.04	0.04	0.04	0.003	0.014	0.29	0.14	n.a.	n.a.	0.07	0.08
FeO	14.85	0.47	4.30	0.23	17.870	0.967	19.46	0.92	0.43	0.16	7.27	0.33
MnO	0.43	0.06	0.13	0.01	1.292	0.365	0.18	0.04	0.00	0.00	0.15	0.03
ZnO	0.00	0.02	0.00	0.00	n.a.		0.04	0.04	n.a.		n.a.	
NiO	0.01	0.01	0.01	0.01	n.a.		0.07	0.04	n.a.		n.a.	
MgO	27.24	0.56	15.61	0.60	11.197	0.775	15.74	0.54	0.16	0.38	15.51	0.45
CaO	0.40	0.20	23.73	0.14	7.237	0.980	0.07	0.04	19.15	0.44	12.11	0.18
Na2O	0.02	0.02	0.29	0.05	n.a.		n.a.		0.62	0.16	2.89	0.14
K2O	0.00	0.01	0.00	0.01	n.a.		n.a.		0.01	0.02	0.09	0.09
Total	99.86	0.46	100.02	0.38	100.503	0.284	99.86	0.40	99.90	0.36	97.34	0.50
	Si	1.920		1.910	Si	2.986	Si	0.070	Si	2.046	Si	6.081
	Al_IV	0.080		0.090	Al_IV	0.014	Al	15.564	Al_IV	1.929	Al_IV	1.919
	Fe_3+	0.000		0.000	Al_VI	1.986	Ti	0.002	Fe_3+	0.017	Ti	0.000
	Al_VI	0.063		0.057	Cr	0.000	Cr	0.048	Ti	0.000	Al_VI	0.783
	Fe_3+	0.016		0.040	Ti	0.003	Fe_3+	0.251	Fe_2+	0.000	Ti	0.079
	Ti_4+	0.001		0.007	Fe_3+	0.012	Fe_2+	3.127	Mn	0.000	Cr	0.008
	Cr	0.001		0.001	Fe_2+	1.101	Mg	4.867	Mg	0.011	Fe_3+	0.307
	Zn	0.000		0.000	Mn	0.082	Mn	0.033	Ca	0.950	Mg	3.308
	Mg	0.919		0.851	Mg	1.243	Zn	0.007	Na	0.055	Fe_2+	0.515
	Fe_2+	0.000		0.046	Ca	0.578	Ni	0.012	K	0.000	Mn	0.000
	Mn_2+	0.000		0.000	T(3)	3.001	Ca	0.016	Z(4)	3.992	Mg	0.000
	Mg	0.539		0.000	M(2)	2.001	R3+	15.935	X(1)	1.017	Fe_2+	0.048
	Fe_2+	0.430		0.046	C(3)	3.004	R2+	8.061	*an*	0.945	Mn	0.018
	Mn_2+	0.013		0.004	*alm*	0.367	Cat(24)	23.996	*ab*	0.055	Ca	1.857
	Ca	0.015		0.929	*sps*	0.027	*Xmg*	0.609	*or*	0.000	Na	0.077
	Na	0.002		0.021	*pyr*	0.414					Na	0.724
	K	0.000		0.000	*grs*	0.185					K	0.016
	T(2)	2.000		2.000	*anr*	0.007					T(8)	8.000
	M1(1)	1.000		1.000	*uvr*	0.000					C(5)	5.000
	M2(1)	1.000		1.000	*Xmg*	0.530					B(2)	2.000
	Xmg	0.772		0.903							A(0-1)	0.740
											Xmg	0.855